



The use of wavelet transform to evaluate the sensitivity of acoustic emission signals attributes to variation of cutting parameters in milling aluminum alloys

Reza Asadi¹ · Seyed Ali Niknam² · Mohamad Javad Anahid² · Iñigo Flores Ituarte¹

Received: 29 November 2022 / Accepted: 20 March 2023 / Published online: 28 March 2023
© The Author(s), under exclusive licence to Springer-Verlag London Ltd., part of Springer Nature 2023

Abstract

Identifying the dominant acoustic emission (AE) signal attributes acquired under various experimental cutting conditions may provide significant insight to the process. Signal processing methods in time-frequency domain are more appropriate for such analysis due to their capabilities to cover the time and frequency transparency and transient phenomena. However, according to the literature, a lack of study was noticed on the sensitivity of AE signal attributes acquired by time-frequency domain analysis to various cutting conditions in the machining processes. Since milling is among the most widely used machining operations, this investigation aims to acquire adequate knowledge about interactions between cutting parameters and their direct and indirect effects on the obtained AE signal attributes from the milling process. To that end, this study investigates wavelet transform (WT) analysis, one of the most famous analyses in the time-frequency domain. WT signal processing was conducted with five models of mother wavelets, and appropriate decomposition numbers were deployed. The detail and approximate signal attributes obtained from each decomposition were assessed. According to WT analysis and statistical calculations, cutting speed, feed rate, and coating material significantly impacted the variation of AE signal attributes. Also, the most sensitive AE signal attributes and decompositions were rms, std, entropy and energy, and 2nd and 6th decompositions, respectively. The outcome of this research can be integrated into artificial intelligence (AI) methods to implement online monitoring and predictive system. Consequently, it may lead to better process control and optimization.

Keywords Acoustic emission · Signal processing · Wavelet transform · Milling · Aluminum 7075

Nomenclature

AE	Acoustic emission
NDT	Non-destructive testing
AI	Artificial intelligence
FEM	Finite element methods
SNR	Signal-to-noise ratio
R^2	Coefficient of determination
MRR	Material removal rate
rms	Root mean square
std	Standard deviation

AA	Aluminum alloy
DWT	Discrete wavelet transform

1 Introduction

Milling is among the most widely used machining processes, which includes a sophisticated morphology and encompasses complicated interactions between cutting parameters, workpiece, and cutting tools [1]. In recent decades, aluminum alloys have been widely applied in numerous industrial sectors and products due to their specific characteristics, including a considerable strength-to-weight ratio, high conductivity, and relatively good machinability [2, 3].

Nowadays, advanced methods and strategies, including AI algorithms, are widely used to analyze sensory signals (e.g., acoustic emission (AE) signals) and improve the efficiency of machining process monitoring [4, 5]. The term AE refers to transient elastic waves obtained from the rapid release of energy from one or more sources when the

✉ Seyed Ali Niknam
saniknam@iust.ac.ir; seyed-ali.niknam@polymtl.ca

¹ Faculty of Engineering and Natural Sciences, Tampere University, Korkeakoulunkatu 6, 33014 Tampere, Finland

² School of Mechanical Engineering, Iran University of Science and Technology, Tehran, Iran

material is under stress [6]. In recent decades, extensive research has been conducted on using AE in various applications. AE also offers significant advantages over other NDT approaches due to its unique ability to monitor manufacturing systems such as power generation, healthcare, offshore and onshore structures, and damage pattern recognition [7, 8]. One of the primary applications of sound signals or AE signals in the machining industry is tool condition monitoring [4]. One of the critical machining processes is milling. It is noteworthy that, in general, the milling process signals are more sophisticated than other non-traditional machining methods. As a result, they are significantly affected by system deviations. These signals can include background noise such as mechanical, electrical, or acoustic. Aluminum alloy machining presents challenges such as burr formation, built-up edge (BUE), and adhesion of work parts to the cutting tools [9–12].

It was assessed whether such signals could be used to monitor and detect critical machining attributes, such as surface roughness, surface quality, tool wear, tool failure, chip thickness, chatter vibration, and tool life [5, 13–21]. Most recent research projects in AE signal usage in machining have focused on AI-based control methods [22–24]. Tool condition monitoring and tool wear measurement using AE signals information are more efficient than ambient signals and vibrations due to the broader range of frequencies AE sensors cover [5, 25]. Knowing their impressive adaption abilities to acquire more satisfying results, researchers have adopted AE signals along with the required sensors and modeling methods in a vast number of recent research in machining and specifically high precision processes [26–28]. Murakami, et al. [26] tried to detect the contact between the cutting tool and workpiece within the micromachining process by using AE signals and built-in AE sensors. Zanger, et al. [28] used FEM simulation and AE signals obtained from piezoelectric sensors for the cutting operation of Ti-Al-4V to evaluate the influence of cutting parameters and analysis of the segmentation frequency of such operations.

Reliable analysis based on AE signals requires parallel consideration of the physical and mechanical conditions of the experiments and an understanding of the signal behavior. AE signals' behavior in machining operations depends on several parameters, such as cutting parameters, tools, and workpiece properties. Besides, the AE attributes in different domains must be well identified and confirmed to enhance the performance and accuracy of the monitoring process [16, 17]. Analyzing the AE signal can be investigated in the time, frequency, and time-frequency AE signals reported in the milling process [29, 30]. In the frequency domain, the conclusions revealed that peak amplitude and peak frequency are the most sensitive factors to input cutting parameters. However, such parameters did not satisfactorily govern them [31]. Various research works on signal processing of the

extracted works are automatic detection [32], surface roughness prediction [33], and modeling slot milling process [30]. Additional studies, including tool wear monitoring in end milling of aluminum-ceramic composites [5] and surface integrity analysis for high-speed machining in the frequency domain [34], were conducted using AE signals attributes. AE signal attributes in the time-frequency domain were also investigated [35].

Although AE signals have significant applications in condition monitoring and health diagnosis of machining processes, there is a lack of research on the time-frequency domain sensitivity of these signals to various cutting parameters. The main characteristics are in milling and high-speed milling as machining processes, the significant effects of interaction, complex chip formation modes, and pressure in different directions. Consequently, the mentioned research deficiencies are more evident in the milling processes, and further studies of AE signal characteristics in the time-frequency domain are needed. By using WT analysis, this study aims to assess the sensitivity of AE signal attributes to cutting conditions in the high-speed milling of 7075-T6 aluminum alloy. Towards this end, a proposed method combined the WT and statistical analyses was deployed. The second section comprises the theoretical background of AE signals. The third section provides the experimental plan. The research methodology was comprehensively discussed in section four. Section 5 consists of the results of the proposed methods and a discussion of them. Finally, the last part presents the conclusion of this research.

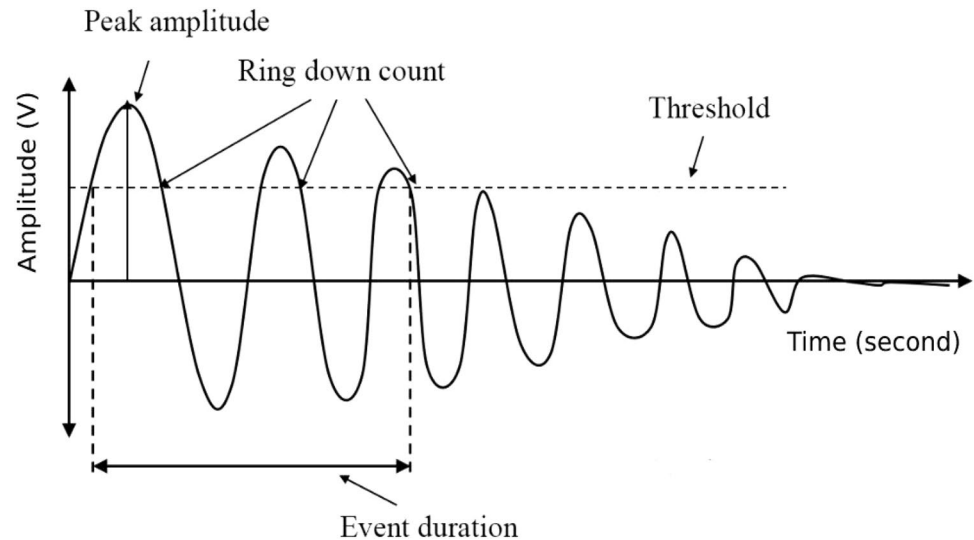
2 Acoustic emission signal

2.1 Definition and sources of AE

In metal machining operations, AE signals are mainly a source of information on plastic deformation and crack generation [36]. The main requirements in this area include AE receivers and sensors, AE signals, AE waveguides, machine tools, background noise, and coupling. Mechanical energy, which is the consequence of releasing elastic waves with a frequency range of 100–1000 kHz, leads to AE signal generation. Generally, piezoelectric sensors detect and convert the generated waves into electrical signals. However, as shown in Fig. 1, each AE event caused by energy dissipation lasts very short (milliseconds range).

2.2 Sources of AE signal

Many studies have evaluated the fundamental sources of AE in deformed/machined materials [37–40]. Based on the reported works, the underlying sources of AE signals in the metal cutting processes are attributed to (a) workpiece plastic

Fig. 1 AE signal attributes [36]

deformation caused during the machining, (b) chip plastic deformation, (c) flank wear caused by friction between the tool flank face and the workpiece, (d) crater wear caused by friction between the tool rake face and chip, (e) chip breakage, (f) tool fracture, and (g) collisions between chip and tool chip breakage. The acquired AE signals from milling processes containing attributes are usually continuous or transient (burst) signals [40]. Tool fracture and chip breakage are undeniable sources of transient signals (Fig. 2) and can be clearly understood to be the result of processes (e) to (g). On the other hand, continuous signals result from deformation and wear on the rake/flank sides of the cutting tools, and the mentioned items (a) to (d) are the key sources of this signal.

2.3 AE parameters

Several attributes can be derived and assessed when processing the wavelet transform of AE signals. Table 1 lists the extracted wavelet transform decomposition-based AE signal attributes. In the Appendix, the formulas of such parameters are provided. Because the behavior of the resulting signals was monitored in a steady state, the features related to such conditions, including max, min, entropy, and energy seem to be more sensitive.

3 Experimental procedures

3.1 Experimental plan

A multilevel full factorial design was constructed in this work to draw the experimental plan. The experimental conditions and their levels are presented in Table 2. The experiments were conducted on a three-axis CNC machine (power:

50 kW, speed: 28,000 rpm; torque: 50 Nm) with the details and levels introduced in Table 2. Notably, 54 ($3^3 \times 2^1$) tests were performed on AA7075-T6 alloy with three types of coated tools. The mentioned 54 tests were repeated three times to guarantee the accuracy and precision of the experimental results. Due to the small difference in the results (around 3%) in all three replications, the average results were used.

To ensure the quality stability of the experimental conditions, preliminary tests were performed, including the strength of cutting processes, tool vibration, and dynamic system behavior. In addition, an AE sensor was installed 2 m from the chip formation zone to investigate the background noise level. The result indicates a high signal-to-noise ratio (SNR), indicating that the background noise has negligible effects on the signals obtained near the chip formation zone (the first sensor). Furthermore, after observing a slight deflection in the workpiece and the cutting tool during the preliminary tests conducted to guarantee the stability of the process and prevent possible tool wear from affecting the AE signals, new inserts were deployed after each machining test. Tables 3 and 4 provide the parameters and attributes of the workpiece and cutting tools. The following section presents the method for this process, including the signal processing method and data analysis.

3.1.1 AE signal monitoring system

Figures 3 and 4 show the AE data acquisition system utilized in this study, including two AE TEDS microphones, a data processing unit, and how the system is set up. Figure 3 shows a comprehensive signal processing unit. The microphones depicted in Fig. 3 b and c were installed near the chip formation zone and at a distance of 2 m from it, respectively. The first microphone was used to obtain AE signals, and the

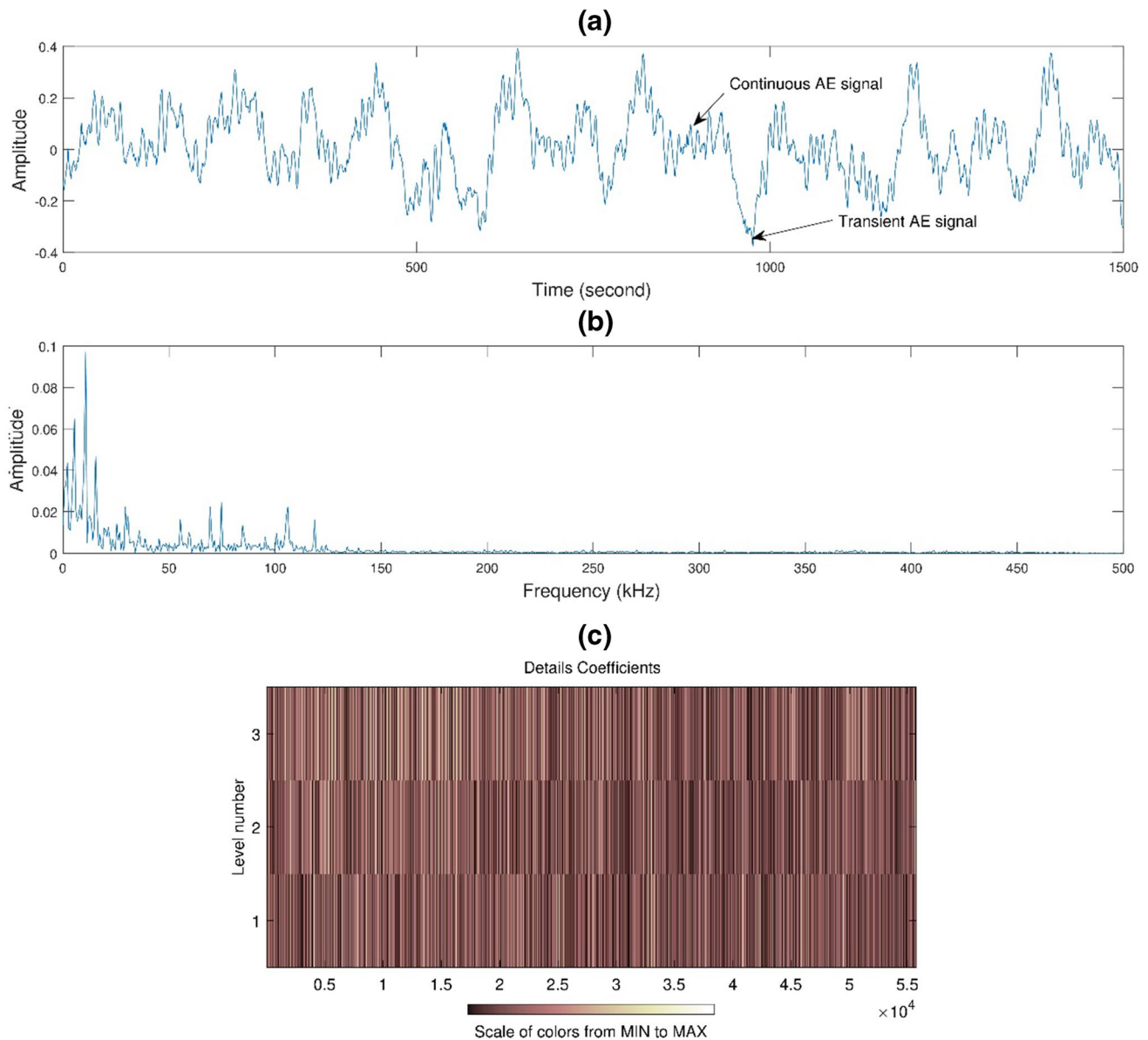


Fig. 2 Samples of AE signal attributes in **a** time domain and **b** frequency domain; **c** wavelet domain with two decompositions

second to measure background noise. The arrangement of the workpieces used during the machining process is shown in Fig. 3d. The schematic view of the experiments is shown in Fig. 4. After implementing the proposed setup, the microphones are calibrated with a signal of $10,000 \pm 100$ Hz to ensure their efficiency and reliability.

3.1.2 Research methodology

Figure 5 shows the required strategy to complete the studies to investigate the effects of cutting parameters on the features of the original AE signals obtained from 0.2 s of cutting operation. The steps of this strategy are as follows:

1. Installation of AE sensors ($f_s = 100$ kHz) near the chip formation zone for data acquisition and Kistler-9255B three-axis dynamometer ($f_s = 48$ kHz) to determine the cutting forces in the coordinate axes. The mentioned dynamometer is utilized to ensure the experiments' accuracy and the experimental conditions' stability.
2. Implementation of milling tests with the proposed conditions and parameters on AA7075-T6 alloy.
3. Obtaining AE time-domain signals ($x(t)$) based on specified cutting parameters used (Fig. 4b).
4. Conversion of time-domain AE signals ($x(t)$) into time-frequency domain data based on the wavelet transform

Table 1 The extracted wavelet features from AE signals

List	AE parameters
1	Maximum: max
2	Minimum: min
3	Root mean square: rms
4	Standard deviation: std
5	Energy: enrg
6	Entropy: entrpy
7	Kurtosis: kur
8	Skewness: skew
9	Crest factor: crest
10	Impulse factor: impulse
11	4th moment: mom4
12	FM4

Table 3 Physical characteristics of the material used [41]

Physical parameters	Materials
	AA 7075–T6
Brinell hardness (HB)	150
Elongation (%)	11
Elastic limit (MPa)	503
Mechanical resistance (MPa) (MPa)	572

Table 4 Parameters of the cutting tools used [42]

Operational conditions	Cutting tool (Iscar Ref: E90A-D.75-W.75-M)		
	TiCN	TiAlN	TiCN + Al ₂ O ₃ + TiN
Insert nose radius <i>Re</i> (mm)	<i>Re</i> = 0.5	<i>Re</i> = 0.83	<i>Re</i> = 0.5
Reference insert	IC 328	IC 908	IC 4050

analysis (DWT_{ψ}^x) and process of obtained AE signals in the time-frequency domain.

- Optimal feature extraction is based on different decompositions (from details and approximated AE signals) and using different mother wavelets.
- Perform statistical analysis to determine the attributes of the processed AE signals with the highest sensitivity to the cutting parameters used in each experiment.

Machining aluminum alloys involves difficulties such as burr formation, BUE, and wear modes, including adhesion [9–12]. Therefore, to minimize the risk of noted challenges and also to avoid the possible negative impacts on the recorded results, the following assumptions are considered:

- The machining process proved stable during the implementation of the preliminary experimental tests performed to validate test conditions. It is noteworthy that cutting tools and fixtures were observed without any deflection. Additionally, there was no chatter vibration detected in the tests.
- New inserts were used at each stage of the designed experiments to avoid the risk of deviations in the test

outcomes and enhance the milling process measurements' accuracy.

The statistical analysis introduced significant parameters, models, decompositions, and mother wavelets by criteria such as *P*-value, R^2 , and R^2_{adj} (Section 3.2).

3.2 Method of analysis

According to the detailed introduction of statistical terms used to analyze data in [43], the following experimental techniques and criteria have been used to identify effective machining parameters on the values of features extracted from wavelet transform signal processing:

- ANOVA: The analysis of variance (ANOVA) assessed any significant relationship between cutting parameters

Table 2 Cutting parameters and their levels used

Cutting parameters	Level		
	1	2	3
A: Cutting speed (m/min)	300	750	1200
B: Feed per tooth (mm/z)	0.01	0.055	0.1
C: Depth of cut (mm)	1	2	-
D: Tool ($D^* = 19.05$ mm, $Z^{**} = 3$)	$R_e = 0.5$ mm Coated with TiCN	$R_e = 0.5$ mm Coated with TiAlN	$R_e = 0.5$ mm Coated with TiCN + Al ₂ O ₃ + TiN
Cutting fluid	None (dry machining)		

D^* tool diameter, Z^{**} tool teeth number

Fig. 3 AE Acquisition system

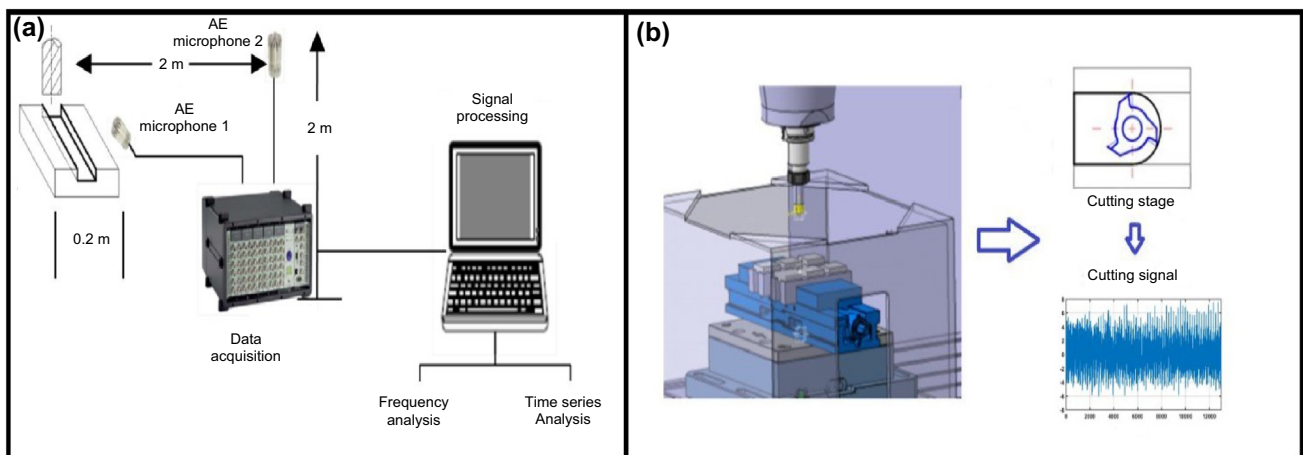
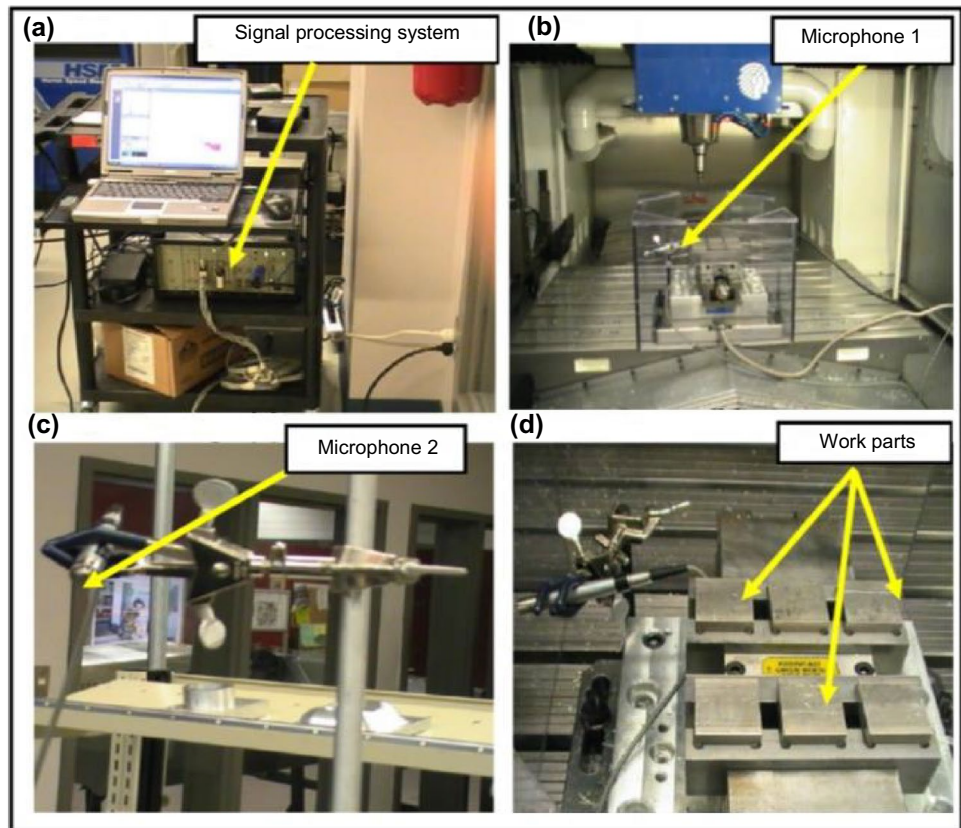


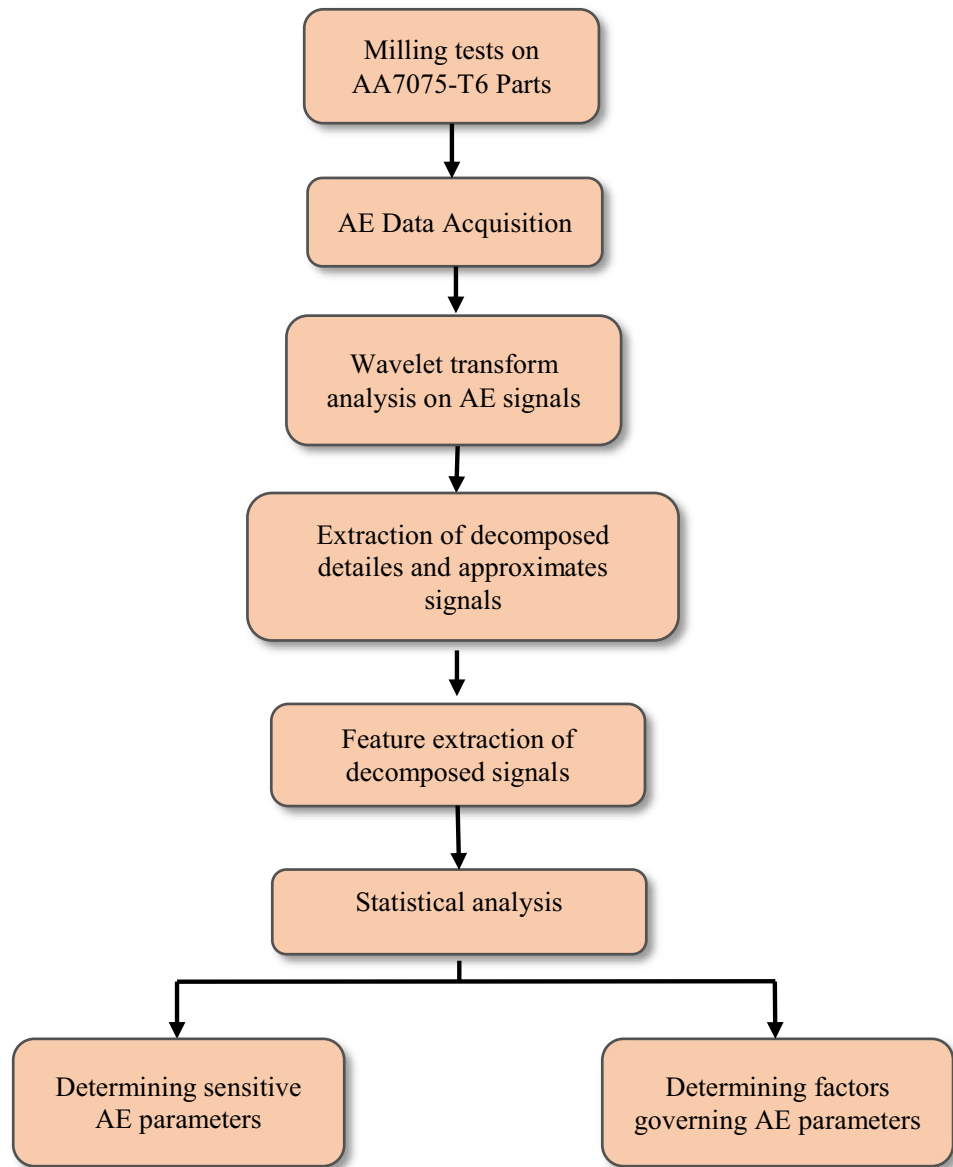
Fig. 4 a The AE signal acquisition system used. b Schematic overview of machining set-up and data acquisition

and obtained AE signal attributes at 95% confidence interval (CI).

- In statistics principles, the coefficient of determination (R^2) indicates the measure of the variability of a dependent variable based on the independent variable(s). Here, this criterion indicates the sensitivity of an extracted AE

feature to a variation of cutting parameters. Whereas $R^2 > 0.85$ indicates significant sensitivity to variation of experimental parameters, $R^2 < 0.85$ shows that the extracted attributes are considered non-sensitive to such parameters.

- R^2_{adj} is a modified version of R^2 and can provide a more detailed view of that correlation. This criterion is equivalent or smaller than R^2 .

Fig. 5 Scheme of the proposed methodology

- *P*-value: Determines whether your experimental test results are statistically significant and is widely used in null-hypothesis significance testing, a statistical method to evaluate if the assumed data proves a hypothesis. This study adopted this criterion to confirm the significance of the cutting parameters and the proposed model based on the linear, second-order degree, or 2-factor interactions. As it was suggested for the first time by Ronald Fisher [44], the following evaluation policy was utilized:
 - P -value < 0.05 ; denotes the proposed model/parameter is significant
 - P -value > 0.1 ; denotes the proposed model/parameter is insignificant
 - $0.05 < P$ -value < 0.1 ; proves that the proposed model/parameter is mid-significant

2. Pareto chart: provides a visual demonstration of statistical analysis of proposed experimental cutting parameters (individual and their combined effects) on the extracted AE signal attributes employing decreasing contribution.

Statistical criteria, including *P*-value, R^2 , and R^2_{adj} , were used to determine the significant and insignificant parameters. It is to say that the models presented in this work are second-order degree models. The AE signal responses with an R^2 less than 0.85 were also insensitive to various cutting parameters as inputs. Also, with magnitudes, less than 0.05 as *P*-value, the cutting parameters and their interactions were considered statistically influential.

4 Results and discussion

After processing the measured AE signals and implementing the strategies for selecting features as described in Fig. 5, an assessment of the sensitivity of the experimental cutting parameters to AE signal attributes was conducted. Five mother wavelets decomposed the measured AE signals: haar, db2, db10, sym8, and bior1.3. After selecting decomposed signals' attributes, a thorough assessment was performed by statistical examinations of the AE attributes. Figure 6 shows maximum R^2 values for the most sensitive signal attributes of the three most significant mother wavelets for approximate and detail signal types. It is worth mentioning that approximate and detail signals are the outcomes of the wavelet transform method, which introduce high and low-frequency decompositions of the milling signals. Based on Fig. 6, the signal attribute "max" (for all three mother wavelets) has the highest R^2 values among all five signal attributes within approximate signals and the lowest for detail signals, having the same R^2 value of about 80% for both approximate and detail signals. The "max" attribute does not differ widely for approximate and detail signals. All four other signal attributes, including rms, std, energy, and entropy, have roughly the same R^2 values for each approximate and detail signal. However, the mentioned four attributes for detail signals have R^2 values 20% more than approximate signals. In other words, the sensitivity of rms, std, energy, and entropy is 20% higher for detail signals. Therefore, regardless of the

mother wavelet type, they were preferred over approximate signals for detecting the changes in machining operations when cutting parameters change. For attribute "max," the second type of mother wavelet (db2) had a better performance. Due to the page limit and long discussion needed, other examined AE signal attributes are not presented in Fig. 6. However, as a brief explanation, it can be claimed that each of the other features evaluated in this study had poorer performance and sensitivity due to a specific reason. For instance, the impulse factor did not significantly affect the signals from the experiments in this paper due to its impact nature. For this reason, displaying features with low R^2 values has been omitted.

Figure 7 summarizes the R^2 values of signal attributes, including rms, std, energy, and entropy for all decompositions and all five mother wavelets studied. Different decompositions do not have the same capability to present sensitive features related to their various details and characteristics. Considering Fig. 7, it can be seen that decompositions 2 and 6 offer higher R^2 values than other decompositions.

As mentioned, R^2 values indicate the variability of a dependent variable based on the independent variable(s). Since different decompositions contain unique details, the results show that decompositions 2 and 6 can introduce the most sensitive features and their required details in the milling of AA 7075. Whereas the R^2 values for different manufacturing processes or alloys may vary, it can be concluded that the appropriate decompositions and features for each unique process can be determined. Thus, it can be easily

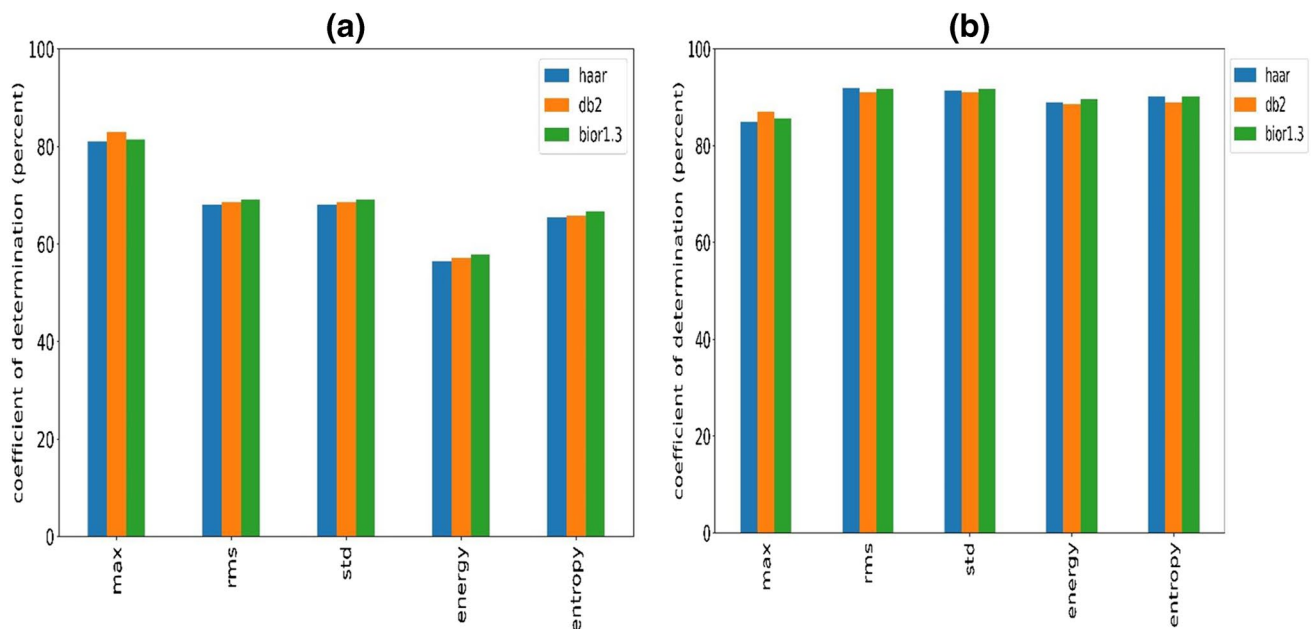


Fig. 6 Coefficient of determination (R^2) calculated for three main mother wavelets for different decompositions: **a** approximate and **b** detail signals

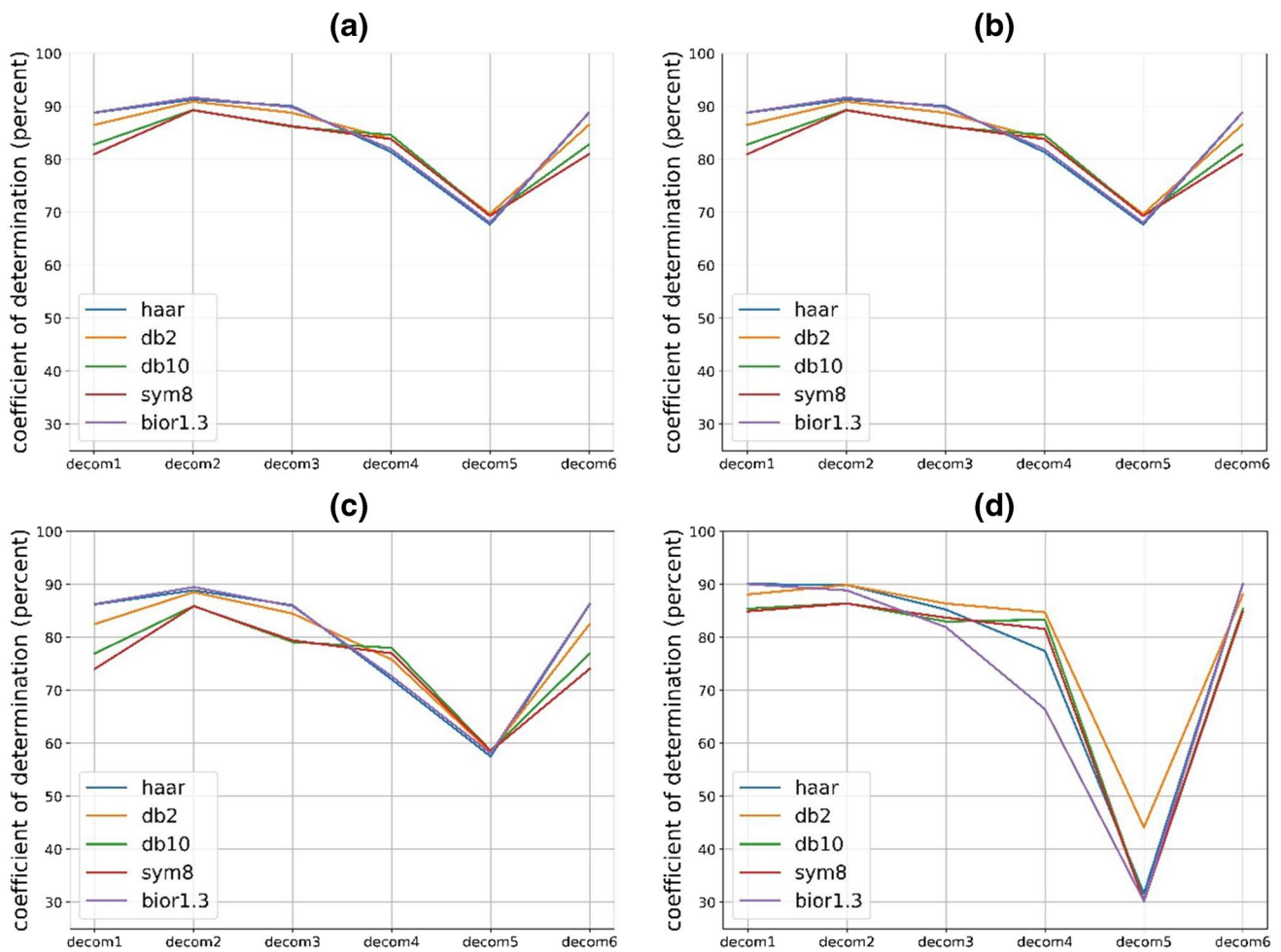


Fig. 7 R^2 changes based on five proposed mother wavelets for **a** rms, **b** std, **c** energy, and **d** entropy as the most sensitive features

understood that rms, std, energy, and entropy in the second and sixth decompositions of detail signals have acceptable sensitivity according to the introduced criteria. Besides, Fig. 6 and Fig. 7 show that R^2 values obtained from the detail signals using the bior1.3, haar, and db2 mother wavelets had the best results, respectively. For further clarification, Table 5 presents the R^2 and R^2_{adj} values of the rms, std, energy, and entropy attributes for decompositions 2 and 6, and bior1.3, haar, and db2 mother wavelets for the detail signals. Except for minor cases where their R^2 was less than acceptable, the bior1.3, haar, and db2 mother wavelets in decompositions 2 and 6 provided sensitive attributes with acceptable accuracy.

Table 6 shows R^2 and R^2_{adj} values for the accumulated detailed signals. It can be observed that the signal resulting from the sum of the detail signals of all decompositions do not provide significant performance. The accumulated detail signal is not separated into different decompositions and includes additional details from the machining process. As a result, it adversely affects the performance of sensitivity

criteria. Figure 8 illustrates the Pareto charts of rms, std, energy, and entropy (features with highest values of R^2) obtained from the most appropriate mother wavelets. Based on the presented charts, rms, std, and energy were substantially controlled with the variation of all the proposed cutting parameters, including the cutting speed (A), feed per tooth (B), coating material (D), and depth of cut (C), respectively, while for entropy, depth of cut (C) cannot be assumed a significant parameter. There is a correlation between the levels of proposed cutting parameters, including cutting speed, feed per tooth, coating strength, and depth of cut (not being effective on entropy level) and rms, std, energy, and entropy, with A as the most effects factor on all the mentioned attributes. The obtained analysis revealed that a considerable proportion of AE signals generated during milling processes are closely linked to consumed energy and material removal rate (MRR) levels, as stated in [45]. Other significant factors on rms and std are the interaction between cutting speeds (AA), coating materials (DD), feed per tooth, and depth of cut (BC). The most observable inputs affecting the entropy are

Table 5 R^2 and R^2_{adj} values of the rms, std, energy, and entropy features for decompositions 2 and 6, using the bior1.3, haar, and db2 mother wavelets

	2nd decomposition						6th decomposition									
	rms		std		Energy		Entropy		rms		std		Energy		Entropy	
	R^2	R^2_{adj}	R^2	R^2_{adj}	R^2	R^2_{adj}	R^2	R^2_{adj}	R^2	R^2_{adj}	R^2	R^2_{adj}	R^2	R^2_{adj}	R^2	R^2_{adj}
Bior1.3	91.459	88.198	91.697	88.998	89.525	86.121	88.894	85.285	89.579	85.942	88.8799	85.2659	86.3223	81.8771	90.0892	86.8682
Haar	91.77	88.45	91.33	88.51	88.91	85.31	89.91	86.61	89.85	86.32	88.84	85.22	86.25	81.78	90.11	86.89
Db2	90.94	87.99	90.45	87.86	88.57	84.86	89.92	86.65	85.32	81.24	86.53	82.152	82.53*	76.85*	88.13	84.27

*Insensitive factors

cutting speed and feed per tooth (AB). However, in comparison to rms and std, the energy was affected by more statistically significant parameters, including coupled interactions between cutting speeds (AA), coating materials (DD), feed per tooth and depth of cut (BC), cutting speed and feed per tooth (AB), cutting speed and depth of cut (AC), and cutting speed and coating materials (AD).

As proved, peak amplitude and peak frequency were not satisfactorily governed by cutting parameters in the frequency domain. The negligible P -value ($\ll 0.05$) of feed per tooth, cutting speed, coating material, and depth of cut when taking rms, std, energy and entropy throughout the wavelet transform analysis of decomposed AE detail signals of milling of aluminum 7075 was observed and considered. It approves that these cutting parameters remarkably control the variation in maximum amplitude. Cutting speed, depth of cut, coating material details, and feed per tooth strongly correlate with AE signals in the time-frequency domain, confirming that AE signals and cutting parameters can be selected appropriately for monitoring machining processes. The order of influential cutting parameters on significant attributes of AE signals was shown in Table 7. Signals obtained from the milling processes are affected by system deviations since they have a more sophisticated nature. Consequently, assessing the sensitivity of signal features and processing the obtained signals play a key role in monitoring and digitizing such processes.

The present study certifies AE signal information’s accuracy and effectiveness in monitoring milling processes. According to the obtained information, it can be claimed that AE signals change more by the variation of cutting parameters (cutting speed and feed per tooth) than by changing the coatings. This study uses a second-order model to investigate the sensitivity of AE signal parameters. As the subject of further studies, evaluating more models for statistical analysis on machining data is suggested. Furthermore, the method introduced in this study can be utilized with AI-based techniques (e.g., neural/deep networks) to develop a robust classification and predictive model and monitor machining operations [46]. Besides, for non-deflecting signals, higher frequency ranges, advanced filtering, and anti-aliasing algorithms are recommended. Finally, it should be noted that the theory of predicting the AE signal parameters is an acceptable approach to avoid the need for repeated tests.

5 Conclusion

A detailed full factorial experimental design with 54 machining tests (milling) on AA 7075 workparts was considered to analyze the obtained AE signals in various process parameters comprehensively. This study would

Table 6 R^2 and R^2_{adj} values of the most significant proposed features using 5 different mother wavelets on accumulated detailed signals

R^2 and R^2_{adj}	Haar		Db2		Db10		Sym8		Bior1.3	
	R^2	R^2_{adj}	R^2	R^2_{adj}	R^2	R^2_{adj}	R^2	R^2_{adj}	R^2	R^2_{adj}
max	82.27	76.51	84.45	79.4	81.09	78.9	83.61	79.25	81.58	75.6
rms	75.87	68.03	78.22	71.14	81.08	74.93	80.87	74.66	75.45	67.48
std	75.87	68.03	78.22	71.14	81.08	74.93	80.87	74.66	75.45	67.48
Energy	66.98	56.25	69.03	58.96	70.99	61.56	70.87	61.4	66.57	55.7
Entropy	76.31	68.61	78.48	71.49	81.64	75.67	81.56	75.57	77.1	69.66

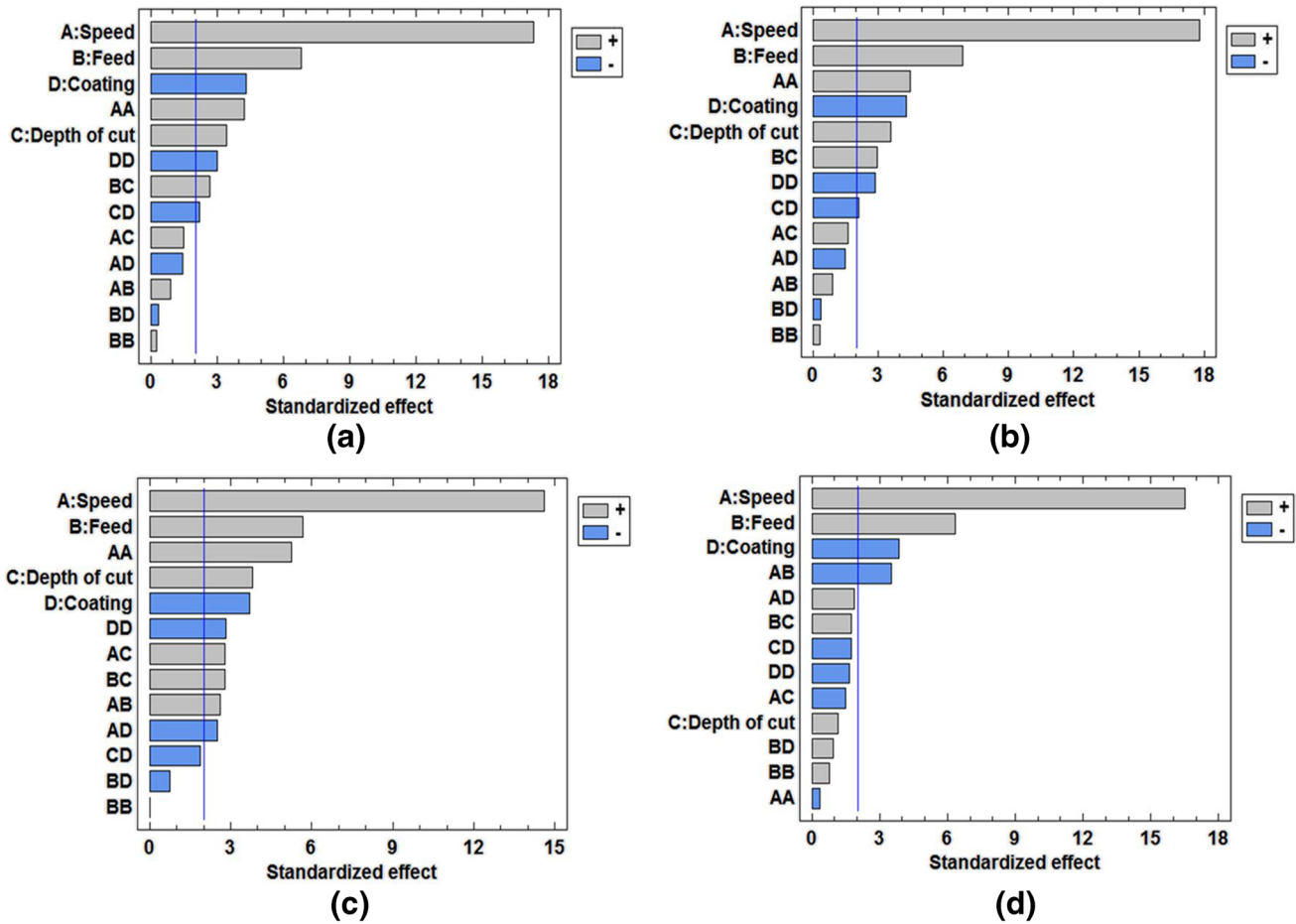


Fig. 8 Pareto charts of sensitive features including **a** rms, **b** std, **c** energy, and **d** entropy with highest values of R^2

Table 7 Effective cutting attributes on sensitive AE parameters

AE parameters	Cutting speed	Feed per tooth	Depth of cut	Coating material
rms	1	2	4	3
Std	1	2	4	3
Energy	1	2	3	4
Entropy	1	2	4*	3

*Non-statically effective factors

illuminate and cover the lack of knowledge about the correlation between the high-speed milling process parameters and significant AE signal attributes derived from time-frequency domain wavelet analysis as a method with high transparency for transient phenomena.

These conclusions could be drawn from the findings presented in the article:

1. Rms, std, energy, and entropy were the most sensitive AE signal attributes to variation of cutting conditions.

2. In decompositions #2 and #6, sensitive AE attributes had higher R^2 values than in other decompositions. It was also noticed that detail signals were more efficient in detecting the variation of cutting conditions and coating material properties compared to approximate signals.
3. Cutting speed, feed per tooth, coating, and cut depth (except in the entropy case) were the most influential factors on rms, std, energy, and entropy. Other significant factors were interaction effects between cutting parameters, with different intensities of influence on each attribute. The mentioned parameters' coupled interaction was the most influential cutting conditions on rms, std, and energy. However, the energy was also influenced by the coupled interaction between cutting speed and feed per tooth, cutting speed and depth of cut, and cutting speed and coating material. Entropy was influenced only by coupled interaction between cutting speed and feed per tooth.
4. As a result of this study, it was demonstrated that AE signals could be used for monitoring milling processes using wavelet domains. Consequently, AE signal information can be used in milling processes, previously denied due to noise, friction, chip accumulation, and lack of accurate extraction and selection of sensory signal attributes.
5. Compared with time and frequency analyses, wavelet transform led to a better determination of sensitive signal features with more accuracy and confidence. Therefore, using the wavelet transform for signal processing is recommended when dealing with high-interaction environments such as machining operations.
6. A combination of AI-based methods, high-quality and precise multiple sensors, a higher frequency range of data, and advanced filtering and anti-aliasing algorithms is suggested to develop the proposed algorithm's efficiency.
7. A comprehensive and precise presentation of significant cutting conditions and sensitive AE signal features to variation input cutting parameters undoubtedly facilitates the predictive fault models and online monitoring systems for diverse machining processes.

Appendix. Description of AE parameters studied

Maximum value of signal, amplitude: max (1)

Average value: mean (2)

$$\text{Mean} = \frac{\sum_{n=1}^N x(n)}{N}$$

Root mean square: rms (3)

$$\text{rms} = \sqrt{\frac{\sum_{n=1}^N (x(n))^2}{N}}$$

Standard deviation : std (4)

$$\text{std}(x(n)) = \sqrt{\frac{\sum_{n=1}^N (x(n) - \text{mean}(x(n)))^2}{N-1}}$$

Energy = $\sum_{n=1}^N (x(n))^2$ (5)

Entropy = $\sum_{n=1}^N \left(x(n) \log \left(\frac{1}{x(n)} \right) \right)^2$ (6)

Kurtosis($x(n)$) = $\frac{\sum_{n=1}^N (x(n) - \text{mean}(x(n)))^4}{(N-1)(\text{std}(x(n)))^3}$ (7)

Skewness($x(n)$) = $\frac{\sum_{n=1}^N (x(n) - \text{mean}(x(n)))^3}{(N-1)(\text{std}(x(n)))^3}$ (8)

Crest factor = $\sqrt{\frac{\max(x(n))}{\frac{\sum_{n=1}^N (x(n))^2}{N}}}$ (9)

Impulse factor = $\frac{\max(x(n))}{\frac{1}{N} \sum_{n=1}^N |x(n)|}$ (10)

Moment4 = $\frac{\sum_{n=1}^N (x(n) - \text{mean}(x(n)))^4}{N-1}$ (11)

FM4 = $\frac{\sum_{n=1}^N \frac{\sum_{n=1}^N (x(n) - \text{mean}(x(n)))^4}{N-1}}{\sum_{n=1}^N \frac{\sum_{n=1}^N (x(n) - \text{mean}(x(n)))^2}{N-1}} = \frac{\text{moment4}}{\text{variance}}$ (12)

Acknowledgements The authors thank the Natural Sciences and Engineering Research Council of Canada (NSERC) and Fonds de recherche du Québec - Nature et technologies (FRQNT).

Author contribution The research results in this work were presented in the B. Sc thesis of Mr. Anahid. Further analysis was added to this work by Mr. Asadi. Dr. Niknam and Dr. Ituarte also acted as advisors on the work. All authors have read and agreed to the published version of the manuscript.

Funding This research has been partially supported by the project Multi-disciplinary Digital Design and Manufacturing - D2M (346874) Academy of Finland (Academy Research Fellow Fund).

Data availability The authors confirm that the data supporting the findings of this study are available within the article and/or its supplementary materials.

Data availability Not applicable.

Declarations

Ethics approval Not applicable.

Consent to participate Not applicable.

Consent for publication All authors permit the publisher to publish the work.

Conflict of interest The authors declare no competing interests.

References

1. Asadi R, Yeganefar A, Niknam SA (2019) Optimization and prediction of surface quality and cutting forces in the milling of aluminum alloys using ANFIS and interval type 2 neuro fuzzy network coupled with population-based meta-heuristic learning methods. *Int J Adv Manuf Technol* 105:2271–2287

2. Sugihara T, Nishimoto Y, Enomoto T (2015) On-machine tool reshaping process for dry machining of aluminum alloys employing LME phenomenon. *Precis Eng* 40:241–248
3. Guo J, Zhang J, Wang H, Liu K, Kumar AS (2018) Surface quality characterisation of diamond cut V-groove structures made of rapidly solidified aluminium RSA-905. *Precis Eng* 53:120–133
4. Gomes MC, Brito LC, da Silva MB, Duarte MAV (2021) Tool wear monitoring in micromilling using support vector machine with vibration and sound sensors. *Precis Eng* 67:137–151
5. Twardowski P, Tabaszewski M, Wiciak–Pikuła M, Felusiak-Czyryca A (2021) Identification of tool wear using acoustic emission signal and machine learning methods. *Precis Eng* 72:738–744
6. Niknam SA, Songmene V, Au YJ (2013) Proposing a new acoustic emission parameter for bearing condition monitoring in rotating machines. *Trans Can Soc Mech Eng* 37:1105–1114
7. Zhu J, He B, Wang X, Cui L, Yuhao L (2018) Extraction of partial discharge signal feature based on dual-tree complex wavelet transform and singular-value decomposition, in: *Cond Monit Diagn (CMD)* 2018:1–5
8. Wei J, Wang H, Lin B, Sui T, Zhao F, Fang S (2019) Acoustic emission signal of fiber-reinforced composite grinding: frequency components and damage pattern recognition. *Int J Adv Manuf Technol* 103:1391–1401
9. Niknam SA, Songmene V (2013) Factors governing burr formation during high-speed slot milling of wrought aluminium alloys. *Proc Inst Mech Eng, Part B: J Eng Manufac* 227:1165–1179
10. Niknam SA, Songmene V (2014) Analytical modelling of slot milling exit burr size. *Int J Adv Manufac Technol* 73:421–432
11. Niknam SA, Songmene V (2015) Burr formation and correlation with cutting force and acoustic emission signals. *Proc Inst Mech Eng B J Eng Manuf* 231:0954405415590562
12. Songmene V, Khettabi R, Kouam J (2012) High speed machining: a cost effective & green process. *Int J Manuf Res (IJMR)* 7:229–256
13. Camara MA, Abrao AM, Rubio JCC, Godoy GCD, Cordeiro BS (2016) Determination of the critical undeformed chip thickness in micromilling by means of the acoustic emission signal. *Precis Eng* 46:377–382
14. Sun S, Hu X, Zhang W (2020) Detection of tool breakage during milling process through acoustic emission. *Int J Adv Manuf Technol* 109:1409–1418
15. Pahuja R, Ramulu M (2019) Surface quality monitoring in abrasive water jet machining of Ti6Al4V–CFRP stacks through wavelet packet analysis of acoustic emission signals. *Int J Adv Manuf Technol* 104:4091–4104
16. Xiao Qi C, Hao Z, Wildermuth D (2001) In-process tool monitoring through acoustic emission sensing. *Autom Mater Proc Group Autom Technol Div* 1
17. Chen X, Li B (2007) Acoustic emission method for tool condition monitoring based on wavelet analysis. *Int J Adv Manuf Technol* 33:968–976
18. Mokhtar N, Ismail IY, Asmelash M, Zohari H, Azhari A (2017) Analysis of acoustic emission on surface roughness during end milling. *ARN J Eng Appl Sci* 12:1324–1328
19. Li Z, Wang G, He G (2018) Surface quality monitoring based on time-frequency features of acoustic emission signals in end milling Inconel-718. *Int J Adv Manuf Technol* 96:2725–2733
20. Sutowski P, Sutowska M, Kapłonek W (2018) The use of high-frequency acoustic emission analysis for in-process assessment of the surface quality of aluminium alloy 5251 in abrasive waterjet machining. *Proc Inst Mech Eng B J Eng Manuf* 232:2547–2565
21. Dib M, Duduch J, Jasinevicius R (2018) Minimum chip thickness determination by means of cutting force signal in micro endmilling. *Precis Eng* 51:244–262
22. Hasan MA, Abu-Bakar M-H, Razuwan R, Nazri Z (2018) Deep neural network tool chatter model for aluminum surface milling using acoustic emission sensor. *MATEC Web Conf* 217:03003
23. Krishnakumar P, Rameshkumar K, Ramachandran K (2018) Machine learning based tool condition classification using acoustic emission and vibration data in high speed milling process using wavelet features. *Int Dec Technol* 12:265–282
24. Elforjani M, Shanbr S (2017) Prognosis of bearing acoustic emission signals using supervised machine learning. *IEEE Transac Indus Electron* 65:5864–5871
25. Abellan-Nebot JV, Subirón FR (2010) A review of machining monitoring systems based on artificial intelligence process models. *Int J Adv Manuf Technol* 47:237–257
26. Murakami H, Katsuki A, Sajima T, Uchiyama K, Houda K, Sugihara Y (2021) Spindle with built-in acoustic emission sensor to realize contact detection. *Precis Eng* 70:26–33
27. Dubey N, Roushan A, Rao U, Sandeep K, Patra K (2018) Tool condition monitoring in micro-end milling using wavelets. In: *IOP Conference Series. Materials Science and Engineering*, p 012045
28. Zanger F, Kacaras A, Bächle M, Schwabe M, León FP, Schulze V (2018) FEM simulation and acoustic emission based characterization of chip segmentation frequency in machining of Ti-6Al-4V. *Procedia CIRP* 72:1421–1426
29. Mohanraj T, Yerchuru J, Krishnan H, Aravind RN, Yameni R (2021) Development of tool condition monitoring system in end milling process using wavelet features and Hoelder's exponent with machine learning algorithms. *Measurement* 173:108671
30. Luo M, Mei J, Zhang D (2016) Time-domain modeling of a cutter exiting a workpiece in the slot milling process. *Chin J Aeronaut* 29:1852–1858
31. Anahid MJ, Heydarnia H, Niknam SA, Mehmanparast H (2020) Evaluating the sensitivity of acoustic emission signal features to the variation of cutting parameters in milling aluminum alloys: Part A: frequency domain analysis. *Proc Inst Mech Eng B J Eng Manuf* 235:0954405420949127
32. Gaja H, Liou F (2016) Automatic detection of depth of cut during end milling operation using acoustic emission sensor. *Int J Adv Manuf Technol* 86:2913–2925
33. Nouhi S, Pour M (2021) Prediction of surface roughness of various machining processes by a hybrid algorithm including time series analysis, wavelet transform and Multi View Embedding. *Measurement* 184:109904
34. Pawade R, Joshi S (2012) Analysis of acoustic emission signals and surface integrity in the high-speed turning of Inconel 718. *Proc Inst Mech Eng B J Eng Manuf* 226:3–27
35. Lee W, Ratnam M, Ahmad Z (2017) Detection of chipping in ceramic cutting inserts from workpiece profile during turning using fast Fourier transform (FFT) and continuous wavelet transform (CWT). *Precis Eng* 47:406–423
36. Tonphong K (2002) Bearing condition monitoring using acoustic emission and vibration, Ph.D. Thesis., Brunel University, UK
37. Lee S, Lee D (2008) In-process monitoring of drilling burr formation using acoustic emission and a wavelet-based artificial neural network. *Int J Produc Res* 46:4871–4888
38. Mian AJ, Driver N, Mativenga PT (2011) Chip formation in microscale milling and correlation with acoustic emission signal. *Int J Adv Manuf Technol* 56:63–78
39. Lee D-E, Hwang I, Valente CM, Oliveira J, Dornfeld DA (2006) Precision manufacturing process monitoring with acoustic emission. In: *Condition Monitoring and Control for Intelligent Manufacturing*. Springer, pp 33–54
40. Rubio E, Teti R, Baciú I (2006) Advanced signal processing in acoustic emission monitoring systems for machining technology. In: *Intelligent Production Machines and Systems*. Elsevier, pp 1–6

41. Niknam SA (2013) Burrs understanding, modeling and optimization during slot milling of aluminium alloys, Ph.D. thesis. École de technologie supérieure, Montreal, Canada
42. Tiabi A (2010) Formation des bavures d'usinage et finition de pièces, M. Sc Thesis, École de technologie supérieure, Montreal, Canada
43. Phadke MS (1989) *Quality engineering using robust design*: Prentice, Hall Englewood Cliffs, NJ
44. Fisher RA (1992) *Statistical methods for research workers*. Springer
45. Dornfeld D (1992) Acoustic emission feedback for precision deburring. *CIRP Annals-Manufac Technol* 41:93–96
46. Jardine A, Lin D, Banjevic D (2006) A review on machinery diagnostics and prognostics implementing condition-based maintenance. *Mech Syst Signal Process* 20:1483–1510

Publisher's note Springer Nature remains neutral with regard to jurisdictional claims in published maps and institutional affiliations.

Springer Nature or its licensor (e.g. a society or other partner) holds exclusive rights to this article under a publishing agreement with the author(s) or other rightsholder(s); author self-archiving of the accepted manuscript version of this article is solely governed by the terms of such publishing agreement and applicable law.